12. Boross, P. and Leusen, J. H. W., Mechanisms of action of CD20 antibodies. *Am. J. Cancer. Res.*, 2012, **2**(6), 676–690.
13. Harjunpaa, A., Junnikkala, S. and Meri, S., Rituximab (anti-CD20) therapy of B-cell lymphomas: direct complement killing is superior to cellular effector mechanisms. *Scand. J. Immunol.*, 2000, **51**, 634–641.
14. USP/MC; Rituximab Summary Validation Report, Report, USP Medicines Compendium, 2013.
15. Reed, G. F., Lynn, F. and Meade, B. D., Use of coefficient of variation in assessing variability of quantitative assays. *Clin. Diagn. Lab. Immunol*., 2002, **9**(6), 1235–1239.
16. Biological Assay Validation. United States Pharmacopoeia, 35–NF 30, 2012.
17. Dafale, N., Semwal, U., Agarwal, P., Sharma, P. and Singh, G., Development and validation of microbial bioassay for quantification of levofloxacin in pharmaceutical preparations. *J. Pharm. Anal*., 2015, **5**(1), 18–26.
18. Coffey, T, Grevenkamp, M., Wilson, A. and Hu, M., Biological assay qualification using design of experiments. *Bioprocess. Int.*, 2013, **11**(6), 42–49.
19. Tsiftsoglou, A. S., Ruiz. S. and Schneider, C. K., Development and regulation of biosimilars: current status and future challenges. *BioDrugs.*, 2013, **27**(3), 203–211.
20. ICH harmonised tripartite guideline, 'Validation on analytical procedures: text and (methodology)', International Council for Harmonisation, Q2 (R1), Step 4, 2005.
21. Design and development of biological assays, United States Pharmacopoeia, 35–NF 30, 2012.

ACKNOWLEDGEMENTS. We thank Central Drugs Standard Control Organization for providing the monoclonal antibody samples. We also thank Dr Renu Jain (Ministry of Health and Family Welfare, Govt of India) for her valuable suggestions and National Institute of Biologicals (Noida) for funds.

Received 17 September 2017; revised accepted 8 March 2018

doi: 10.18520/cs/v114/i12/2513-2518

# Improved square-Z-shaped DNG meta-atom for C- and X-band application

**Md. Mehedi Hasan[1], Mohammad Rashed Iqbal Faruque[1,*] and Mohammad Tariqul Islam[2]**

[1]Space Science Centre (ANGKASA), Universiti Kebangsaan Malaysia, Bangi 43600, Malaysia
[2]Department of Electrical, Electronic and Systems Engineering, Universiti Kebangsaan Malaysia, Bangi 43600, Malaysia

**An improved dual-band square-Z-shaped meta-atom is presented. It shows a bandwidth of 3.61 GHz, where the operating frequency ranges from 2.0 to 14.0 GHz. The meta-atom is split in such a way that it appears as a square-Z-shaped structure and is printed on an epoxy resin fibre substrate material. The dimensions of the single unit cell and array structure are respectively, 10 × 10 mm$^2$ and 200 × 150 mm$^2$. Also the unit cell and 1 × 2, 2 × 2 and 4 × 4 arrays are studied for double negative characteristics. CST Microwave Studio 3D-electromagnetic simulator is used to design and perform investigation. The performance of a meta-atom unit cell is measured by wave guide ports. The measured and simulated results matched well and are applicable for C- and X-band applications.**

**Keywords:** Double negative meta-atoms, dual-band, effective medium ratio.

META-ATOMS are artificially engineered resonant materials able to manipulate light at a sub-wave length scale. They can be designed to strongly interact with the electric and/or magnetic fields of incident electromagnetic (EM) waves, thus enabling many unique properties (e.g. perfect absorption, sub-wavelength focusing and negative refractive index). Split-ring resonators are commonly used elements in meta-atoms and can generate a magnetic response that gives a negative permeability. Double negative meta-atoms offer the possibility to obtain certain exotic properties. With considerable efforts, progress has been made towards the realization of high-performance double negative meta-atom with wide operation bandwidth and dynamic EM properties. In 1968, Veselago[1] described the negative permittivity and permeability that showed certain peculiar characteristics of waves, even though no physical material or device was found having negative $\varepsilon$ and $\mu$ until 1999, when Pendry et *al.*[2] proposed periodically stacked split ring resonators (SRRs) at microwave frequencies which exhibited simultaneous negative $\varepsilon$ and $\mu$. Since then, many studies have been reported on related topics of perfect lenses, and potential applications in lenses, absorbers, antennas, optical and microwave components and sensors. In 2000, Smith *et al.*[3] introduced a material that simultaneously showed negative permittivity and negative permeability, with some exceptional characteristics at microwave frequencies. Owing to unusual characteristics of meta-atoms when compared to conventional materials, meta-atoms can be applied in numerous applications such as, EM-band gap structures[4], EM-absorption[5], enhanced antenna performances, polarization resonators, solar energy harvesters and super lenses. Although negative permittivity occurs in some natural conventional materials, negative permeability is hard to observe in natural materials and DNG characteristics are difficult to obtain. To meet the requirements of particular applications, several letter-shaped meta-atoms were discussed earlier. Hasan *et al.*[6] presented a z-shaped DNG, which had wide bandwidth. The dimension of the metamaterial single unit cell was 10 × 10 mm$^2$ and applicable for dual band applications. A square split z-shape meta-atom was applicable for S-, C-,

*For correspondence. (e-mail: rashed@ukm.edu.my)

**Table 1.** Design specifications of square-*Z*-shaped meta-atom unit cell

| Parameter specifications | Dimension (mm) | Parameters specifications | Dimension (mm) |
|---|---|---|---|
| *a* (substrate material wide) | 10.0 | *d* (metal strip wide) | 0.50 |
| *b* (substrate material length) | 10.0 | *g* (split wide) | 0.50 |
| *L* (unit cell length) | 8.0 | *t* (substrate material thickness) | 1.60 |
| *W* (unit cell wide) | 8.0 | *h* (copper thickness) | 0.035 |

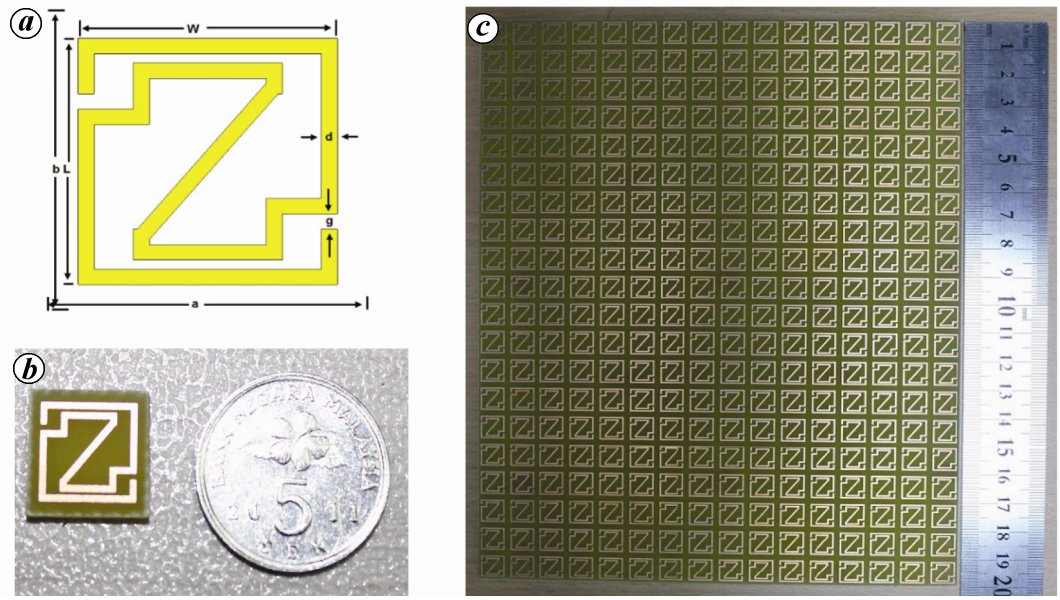


**Figure 1.** Schematic illustration of the geometry (***a***) and fabricated (***b***) (10 × 10 mm$^2$) meta-atom unit cell structure and (200 × 160 mm$^2$) meta-atom array structure used for measurement (***c***).

X- and Ku-band applications and analysed at different azimuthal angles like, $\pi/12$, $\pi/6$, $\pi/4$, $\pi/3$, $5\pi/12$, and $\pi/2$ (ref. 7). In Chun *et al.*[8] a $\pi$-shaped (pi-shaped) metamaterial was presented. The basic configuration contains two symmetrical $\pi$-shaped structures connected by a copper strip where the $\pi$-shaped structure was formed by symmetrical metallic *C*-shaped resonator and continuous wire. The metamaterial showed double negative property in conjunction with negative permittivity and permeability from the frequency 11.20 GHz to 13.05 GHz that covered the little portion of X and Ku-band. Liu *et al.*[9] designed a single-sided left-handed metamaterial that showed resonance at X-band and negative permittivity from 10.20 to 11.70 GHz, as well as the negative permeability from 10.20 to 11.40 GHz. Therefore, the left handed pass band of the designed MCER was from 10.20 to 11.40 GHz. Urbani *et al.*[10] proposed a left-handed diamond-shaped metamaterial that exhibited an increased receive power and transmission peak. Hossain *et al.*[11] suggested an *S*-shaped DNG metamaterial for S- and C-band applications. They designed a unit cell and arrays of several dimensions and explained the effect of size on the resonance frequency. A compact dual band meta-atom was designed as 'delta-shaped' on Rogers RT 5880 dielectric materials for C-band applications[12]. The 7.50 × 7.50 mm$^2$ delta shaped electric meta-atom was designed by integrating with a rectangular close ring resonator and the effective medium ratio was around 7.10. Hasan *et al.*[13] presented an inverse *E*-shape DNG chiral metamaterial printed on Rogers RT 5880 material and exhibited 5.14 GHz bandwidth from 4 to 9.14 GHz.

The square-*Z*-shaped structure proposed in this study shows dual band resonances with negative refractive index bandwidths of 3.61, 2.17 and 2.41 GHz respectively, for the frequency regions of 3.48–7.09 GHz, 7.87–10.04 GHz and 11.59–14.0 GHz. The bandwidth of 3.61 GHz is greater than that reported earlier[8,12,13]. In addition, the proposed structure's unit cell dimensions are 10 × 10 mm$^2$, which are smaller than those in other studies[10,11]. Because the effective medium ratio is larger than 4, the structure is flexible enough for practical implementation in applications such as antennas, EM-filters and EM-cloaking devices.

The meta-atom structure is composed by combining the two ring resonators with an arrangement of splits and metal strips. The inner resonator is bent like a *Z*-shaped structure. Therefore, the whole meta-atom structure looks like a square-*Z*-shaped split-ring resonator of copper metal strips and the design specifications are given in Table 1. Epoxy resin fibre with permittivity of 4.50 and

thickness of 1.60 mm is used as substrate material. All the designs, simulations and investigations were obtained through CST Microwave Studio software. The designed square-*Z*-shaped $10 \times 10$ mm$^2$ meta-atom unit cell and $200 \times 150$ mm$^2$ array are displayed in Figure 1.

Electromagnetic simulation helps in evaluating the fundamental field quantities from Maxwell's equation, adopting some numerical methods. It explains the electromagnetic wave propagation and interactions with meta-atoms. To design and study precise electromagnetic structures, selection of simulation software is indispensable before the prototyping process. The finite-integration-technique-based CST Microwave Studio is used to obtain the results. Figure 2 shows the setup of a *Z*-shaped meta-atom, where the meta-atom is placed between wave guide ports parallel to the *z*-axis, where electromagnetic waves are incident from the positive to negative direction of the *z*-axis. Boundary conditions are usually used in most computer simulations to speed up the computation process. Electric conductor and magnetic conductor boundaries are applied along the *x* and *y* axes respectively. These boundary conditions are given advantages to decrease cross section sizes, simplify material communication contemplations and speedup calculation times.

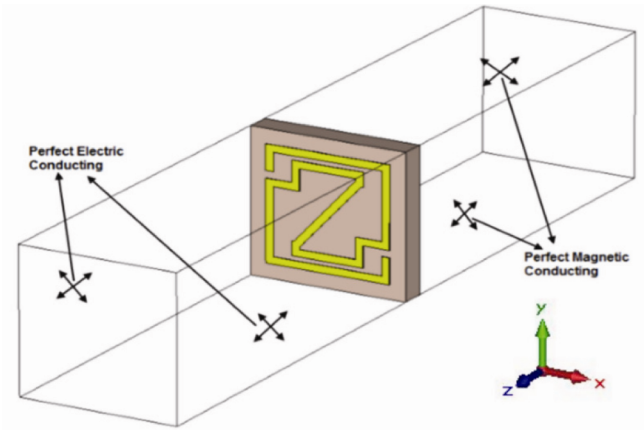


**Figure 2.** Simulation setup of *Z*-shaped meta-atom in CST microwave studio.

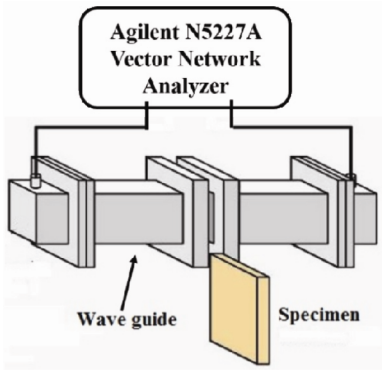


**Figure 3.** Measurement arrangement for *S*-parameters.

For measurement purposes, a $10 \times 10$ mm$^2$ single unit cell and $200 \times 150$ mm$^2$ array prototype were fabricated. The measurement of meta-atom is performed according to the wave guide port method. For the measurement of the designed meta-atom, two rectangular waveguides are utilized according to the simulation setup. The wave guides are connected to the Agilent N5227A vector network analyser (VNA) by the semi-rigid coaxial cable and connectors. The Agilent N5227A VNA is equipped with two measurement ports and capable of measuring from 10 MHz to 67.0 GHz. For error free measurement, calibration prior to measurement is required. An Agilent N4694-60001 electronics calibration module has been used to calibrate the Agilent N5227A vector network analyser. The wave guides work as transmitting and receiving ends. The fabricated prototype is placed between the transmitter and receiver wave guide and the reflection and transmission coefficients are measured. The measurement setup for the proposed meta-atom is displayed in Figure 3.

The reflection and transmission coefficients associated with the EM-properties of the proposed meta-atom are calculated[14], where $S_{11}$ and $S_{21}$ depend on the proposed meta-atom dimension. However, the reflection ($\Gamma$) is explained as

$$\Gamma = \left\{ \frac{(Z_0 - 1)}{(Z_0 + 1)} \right\}, \tag{1}$$

$$Z_0 = \left( \sqrt{\frac{\mu_r}{\varepsilon_r}} \right). \tag{2}$$

The reflection ($S_{11}$) and transmission ($S_{21}$) parameters are expressed as

$$S_{11} = \left\{ \frac{(1 - \Gamma^2)Z}{(1 - \Gamma^2 Z^2)} \right\}, \tag{3}$$

$$S_{21} = \left\{ \frac{(1 - Z^2)\Gamma}{(1 - \Gamma^2 Z^2)} \right\}, \tag{4}$$

where $Z = \exp\{-j((2\pi f/c)\sqrt{\varepsilon_r \mu_r d})\}$. Nicolson–Ross–Weir method (NRW method) is adopted for the characterization of meta-atom because it provides easy evaluation of permittivity and permeability from the transmission and reflection coefficients as well as avoids determination of the cosine branch index. Thus, the effective permittivity ($\varepsilon_r$), permeability ($\mu_r$) and refractive index ($n_r$) are given by

$$\varepsilon_r = \left\{ \frac{c}{j\pi fd} \times \frac{(1 - S_{21} - S_{11})}{(1 + S_{21} + S_{11})} \right\}, \tag{5}$$

$$\mu_r = \left\{ \frac{c}{j\pi fd} \times \frac{(1 - S_{21} + S_{11})}{(1 + S_{21} - S_{11})} \right\}, \tag{6}$$

$$n_r = \left[ \frac{c}{j\pi fd} \sqrt{\left\{ \frac{(S_{21} - 1)^2 - S_{11}^2}{(S_{21} + 1)^2 - S_{11}^2} \right\}} \right]. \tag{7}$$

The meta-atom construct by lumped element and resonance points at

$$f = \frac{1}{2\pi\sqrt{L_T C_T}}. \tag{8}$$

EM-wave propagation along the meta-atom unit cell and coupling between the splits and the electric field produce electric resonances. Further, coupling between the magnetic field and the loops produces magnetic resonances. The total inductance ($L_T$) of the proposed meta-atom is approximated as[15]

$$L_T = 0.01 \times \mu_0 \left\{ \frac{2(d + g + h)^2}{(2w + g + h)^2} + \frac{\sqrt{(2w + g + h)^2 + l^2}}{(d + g + h)} \right\} t. \tag{9}$$

The total capacitance ($C_T$) is obtained as

$$C_T = \varepsilon_0 \left[ \frac{(2w + g + h)}{2\pi(d + h)^2} \ln\left\{ \frac{2(d + g + h)}{(a - l)} \right\} \right] t, \tag{10}$$

where the free-space permittivity ($\varepsilon_0$) is $8.85 \times 10^{-12}$ F/m and permeability ($\mu_0$) is $4\pi \times 10^{-7}$ H/m.

To obtain a wider negative refractive index bandwidth, the inductance and capacitance are formed in the series and shunt branches of the circuit diagram. The splits are maintained by the capacitive effect and produce little phase delay, which are symbolized as $C_1$, $C_2$, $C_3$, $C_4$ and $C_5$. Further, inductive effects are formed by the metal strips, which are labelled $L_1$, $L_2$ and $L_3$. Figure 4 *a* shows the equivalent circuit of the proposed structure and the current distribution at 11.84 GHz is presented in Figure 4 *b*. Current in the opposite direction on the inner and outer surfaces of the resonator owing to the dissimilar geometries of structure causes the stop band.

The scatterings and effective medium parameters of a single meta-atom structure and arrays are studied to comprehend the characteristics of a meta-atom.

The numerically calculated and experimental magnitudes of the reflectance and transmittance are revealed in Figure 5 *a* and *b* respectively. In Figure 5 *b*, the simulation result shows resonances at 7.32 and 11.84 GHz, whereas the measured resonances appear at 7.53 and 12.02 GHz. Moreover, the measured transmittance result is slightly shifted and smaller than the simulated value. Figure 5 *c* shows the negative frequency band of permeability from 8.13 to 14.0 GHz (bandwidth of 5.87 GHz) and negative permittivity from 4.05 to 10.37 GHz and 13.38 to 14.44 GHz. The variation between the permeability, permittivity and refractive index for the polarization effect in the material internal structure as well as amplitude of the effective medium parameters are shifted by changing the structural design of the meta-atom. It was noted that the refractive index is negative when permittivity and permeability are simultaneously negative for double negative characteristics. From Figure 5 *c*, the refractive index is negative from 3.48 to 7.09 GHz, 7.87 to 10.04 GHz and 11.59 to 14 GHz. Therefore, at 8.79 GHz, the magnitudes of effective permittivity, permeability and refractive index are respectively, –8.35, –34.92 and –16.04. Thus, the meta-atom is said to be a double negative meta-atom.

Open arrays with dimensions of 1 × 2, 2 × 2 and 4 × 4 are analysed to study the DNG characteristics by measuring the effective medium parameters.

The reflectance ($S_{11}$) and transmittance ($S_{21}$) of the square-*Z*-shaped 1 × 2 array is shown in Figure 6 *a* and *b* respectively. Figure 6 *b* shows that at resonance frequencies of 7.52, 11.38, and 13.43 GHz, $S_{21}$ is –28, –21 and –22 dB respectively. According to Figure 6 *c*, negative permeability appears from 7.93 to 14.0 GHz as well as refractive index is negative from 3.38 to 7.34 GHz, 7.80 to 10.25 GHz and 11.13 to 12.52 GHz for the 1 × 2 array configuration. In addition, the 1 × 2 array structure clearly exhibits DNG properties at 8.60 GHz, where the absolute magnitudes are –5.45 (permittivity), –29.83 (permeability) and –13.19 (refractive index).

To study the 2 × 2 array configuration, the same methodology is followed to obtain the values of $S_{11}$ and $S_{21}$ and calculate effective medium parameters of the 2 × 2 array. Figure 7 *a* and *b* shows the magnitudes of $S_{11}$ and $S_{21}$. Figure 7 *b* shows that at the resonance frequencies, 6.28, 7.73, 8.91, 11.14, 12.94 and 13.37 GHz, $S_{21}$ is –18.43, –22.05, –23.25, –18.36, –12.95, and –26.11 dB respectively. The real amplitudes of permittivity and permeability are displayed in Figure 7 *c*. Here, the permeability shows a negative band of frequencies from 7.89 to

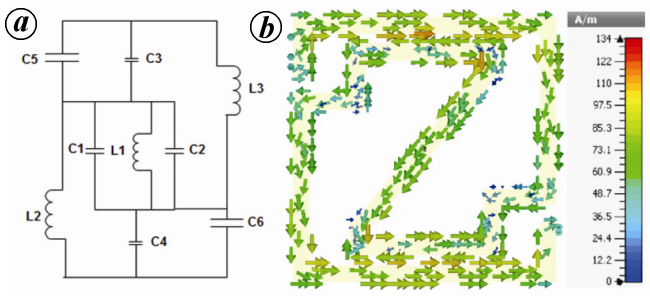


**Figure 4.** ***a***, Lumped circuit diagram of the square-*Z*-shape structure, ***b***, Surface current distribution at 11.84 GHz.

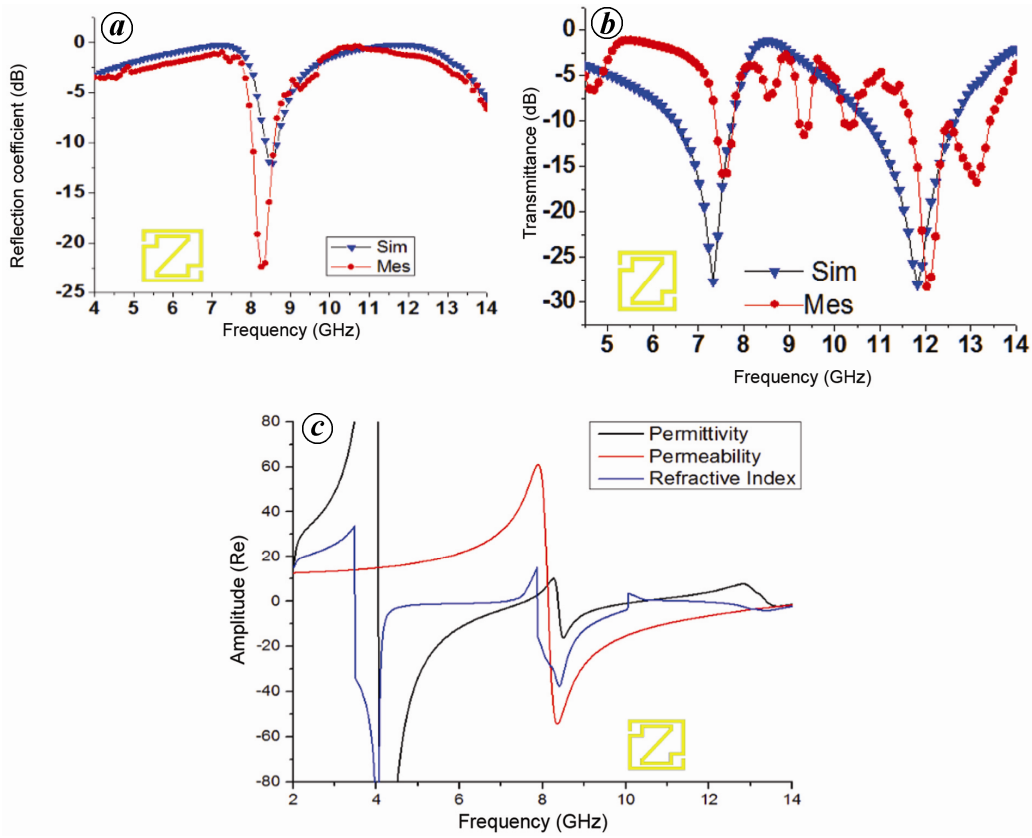


**Figure 5.** Magnitude of (***a***) reflection ($S_{11}$) coefficient in units of dB, (***b***) transmission ($S_{21}$) coefficient in units of dB, and (***c***) effective medium parameters versus frequency for square-*Z*-shaped meta-atom.

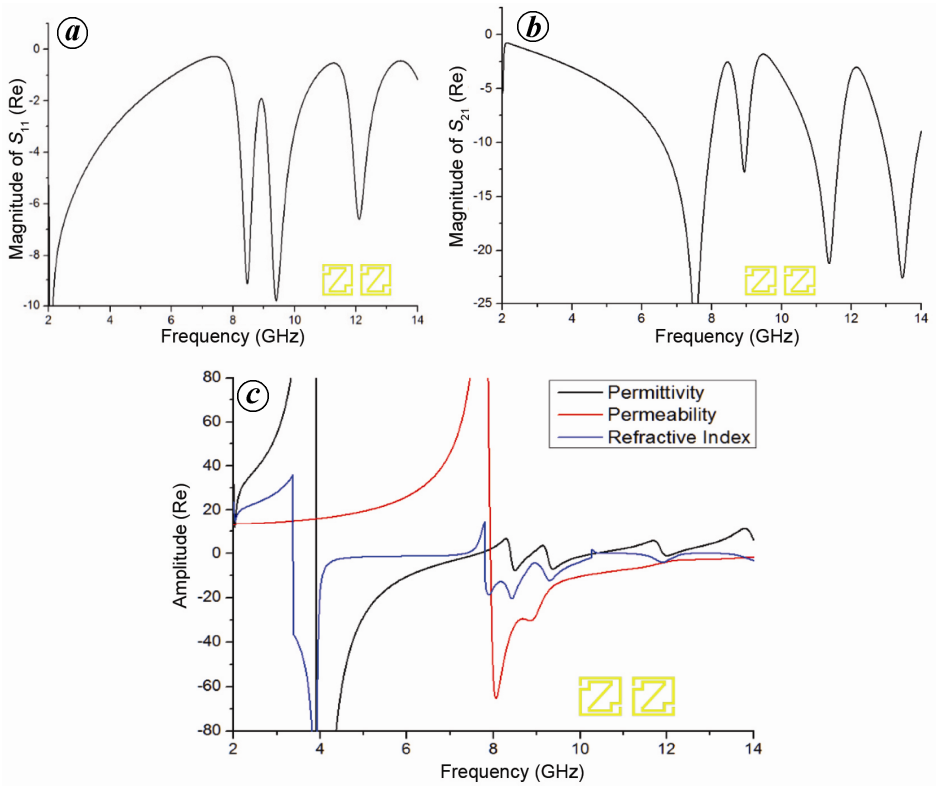


**Figure 6.** Magnitude of (***a***) reflection ($S_{11}$) coefficient in units of dB, (***b***) transmission ($S_{21}$) coefficient in units of dB, and (***c***) effective medium parameters versus frequency for 1 × 2 array structure.

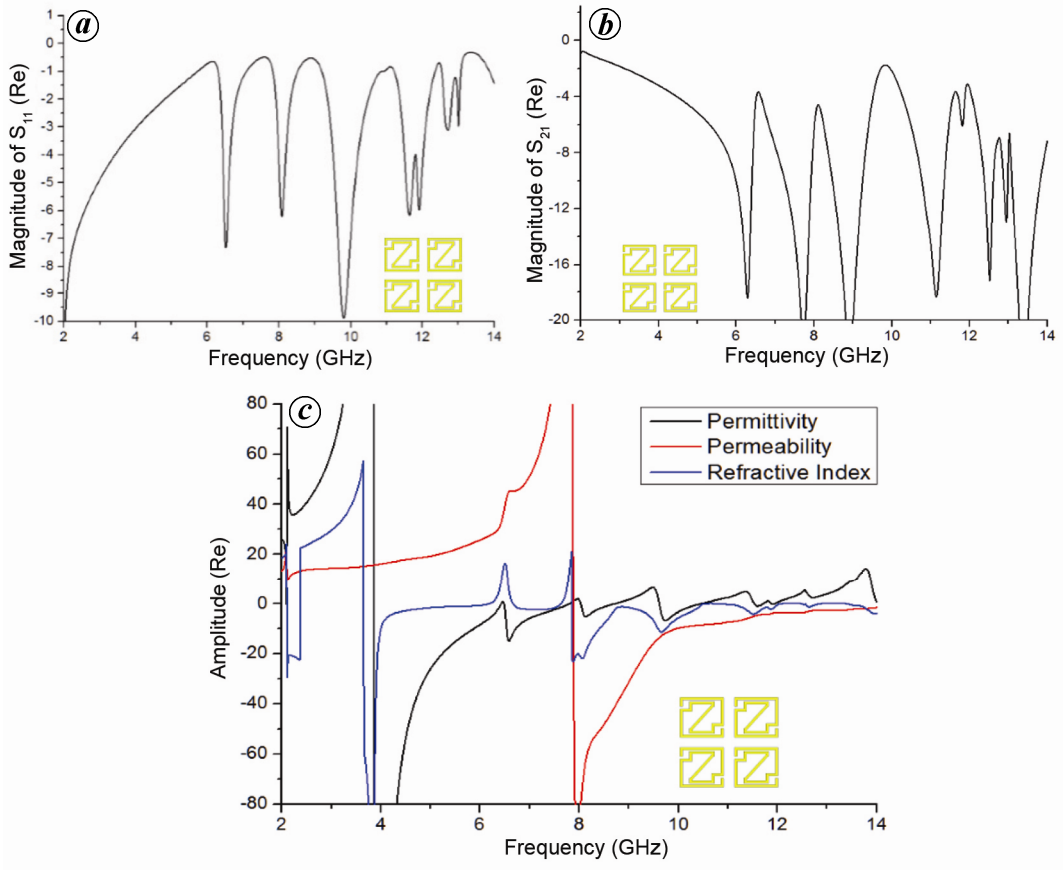


**Figure 7.** Magnitude of (***a***) reflection ($S_{11}$) coefficient in units of dB, (***b***) transmission ($S_{21}$) coefficient in units of dB, and (***c***) effective medium parameters versus frequency for 2 × 2 array structure.

**Table 2.** Characterization of unit cell and arrays of proposed meta-atom

| Structures | Frequency (GHz) | Permittivity ($\varepsilon$) | Permeability ($\mu$) | Refractive index ($n$) | Effective medium ratio | Meta-atom type |
|---|---|---|---|---|---|---|
| Single unit cell | 8.79 | –8.35 | –34.04 | –16.92 | 4.1 | DNG |
| 1 × 2 array | 8.60 | –5.45 | –29.83 | –13.19 | 4.0 | DNG |
| 2 × 2 array | 8.60 | –0.68 | –45.04 | –5.55 | 4.7 | DNG |
| 4 × 4 array | 8.60 | –4.17 | –31.75 | –12.80 | 4.0 | DNG |

**Table 3.** Comparison between the sizes of designed meta-atom with existing structures

| References | Year | Dimension ($mm^3$) | Meta atom type |
|---|---|---|---|
| Urbani *et al.*[10] | 2010 | 20 × 25 × 0.25 | DNG |
| Hossain *et al.*[11] | 2015 | 12 × 12 × 0.80 | DNG |
| Sarkhel *et al.*[12] | 2015 | 7.5 × 7.5 × 1.57 | SNG |
| Proposed meta-atom | 2017 | 10 × 10 × 1.60 | DNG |

14.0 GHz and in case of permittivity, shows a negative band of frequencies from 3.86 to 7.79 GHz and 8.03 to 8.71 GHz in the microwave region. In Figure 7 *c*, negative frequency region of the refractive index from 3.65 to 6.17 GHz and 7.85 to 10.54 GHz as well as at 8.60 GHz and the 2 × 2 array shows DNG characteristics.

Figure 8 *a* shows the amplitude of transmission ($S_{21}$) coefficient of the 4 × 4 array structure, and the permeability, permittivity and refractive index are shown in Figure 8 *b*. Figure 8 *a* shows that at 7.53, 11.0 and 12.56 GHz, resonance frequency amplitudes are –27, –21.31, and –16 dB respectively. According to Figure 8 *b*, negative permeability appears from 7.94 to 14.0 GHz. Again, the array structure exhibits negative refractive index from 3.26 to 7.36 GHz and 7.82 to 10.01 GHz. The bandwidth of more than 4.0 GHz is notable.

Table 2 lists the effective medium parameters of the designed unit cell and array configuration. Here, the effective medium parameters show little difference

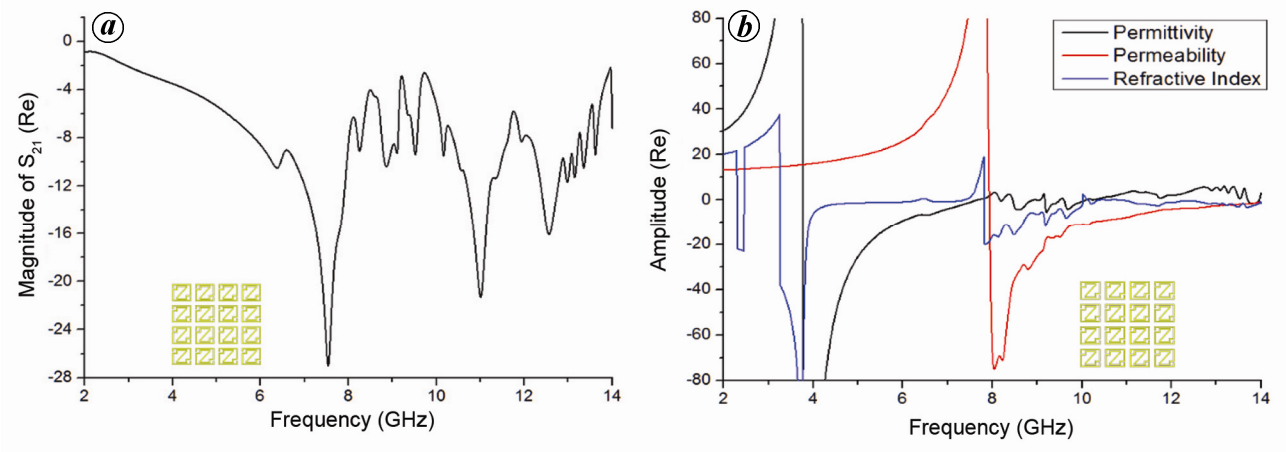


**Figure 8.** Magnitude of the (***a***) transmission ($S_{21}$) coefficient in units of dB and (***b***) effective medium parameters versus frequency for 4 × 4 array structure.

between the unit cell and the arrays but both exhibit the DNG characteristics. The effective medium ratio for all structures are larger than 4.0, indicating that the proposed structure is compact in size and can be used in many sophisticated applications such as EM-cloaking, enhancement of antenna performance, filter design, noise reduction, sensing and detection systems and imaging systems.

The dimensions are an important factor affecting the compactness of the meta-atom. Table 3 compares the dimensions of the proposed meta-atom with those of previously reported structures from the literature. The proposed meta-atom dimension is more compact than the reported structure dimensions[10,11]. Sarkhel *et al.*[12] reported a SNG metamaterial with a thickness of 1.575 mm. However, if the unit cell thickness is less than 1.0 mm, the structure is called a two-dimensional meta-atom.

An improved square-*Z*-shaped meta-atom structure exhibits DNG properties over a wide bandwidth covering much of the C- and X-band. Experimental results show that the proposed meta-atom shows a bandwidth of more than 3.6 GHz and an effective medium ratio of more than 4; these results are more current than the reference prototypes. Therefore, the square-*Z*-shaped DNG meta-atom is applicable in modern radio systems and GEO satellite communication, as the C- and X-band are relevant for weather radar monitoring and vehicle speed detection for law enforcement. In addition, by integrating this proposed meta-atom into an antenna, a favourable gain, bandwidth, and miniature antenna for C- and X-band application can be obtained.

1. Veselago, V. G., The electrodynamics of substances with simultaneously negative values of $\varepsilon$ and $\mu$. *Sov. Phys.*, 1968, **10**, 509–514.
2. Pendry, J. B., Holden, A. J., Robbins, D. J. and Stewart, W. J., Magnetism from conductors and enhanced nonlinear phenomena. *IEEE Trans. Microw. Theory Technol.*, 1999, **47**, 2075–2084.
3. Smith, D. R., Padilla, W. J., Vier, D. C., Nemat-Nasser, S. C. and Schultz, S., Composite medium with simultaneously negative permeability and permittivity. *Phys. Rev. Lett.*, 2000, **84**, 4184–4187.
4. Barth, S. and Iyer, A. K., A miniaturized uniplanar metamaterial-based EBG for parallel-plate mode suppression. *IEEE Trans. Microw. Theory Technol.*, 2016, **64**(4), 1176–1185.
5. Sarkhel, A. and Chaudhuri, S. R. B., Compact quad-band polarization insensitive ultrathin metamaterial absorber with wide angle stability. *IEEE Antennas. Wirel. Propag. Lett.*, 2017; doi:10.1109/LAWP.2017.2768077.
6. Hasan, M. M., Faruque, M. R. I., Islam, S. S. and Islam, M. T., A new compact double-negative miniaturized metamaterial for wide-band operation. *Materials*, 2016, **9**(10), 830.
7. Hasan, M. M., Faruque, M. R. I. and Islam, M. T., Left-handed metamaterial using *Z*-shaped SRR for multiband application by Azimuthal angular rotations. *Mater. Res. Exp.*, 2017, **4**(4), 1–11.
8. Chang-Chun, Y., Yi-Ping, C., Qiong, W. and Shing-Chuang, Z., Negative refraction of a symmetrical $\pi$-shaped metamaterial. *Chin. Phys. Lett.*, 2008, **25**(2), 482–484.
9. Liu, S. H., Guo, L. X. and Li, J. C., Left-handed metamaterials based on only modified circular electric resonators. *J. Mod. Opt.*, 2016, **63**(21), 2220–2225.
10. Urbani, F., Experimental analysis of novel single-sided left-handed metamaterial. *IEEE Antennas Wirel. Propag. Lett.*, 2010, **9**, 720–723.
11. Hossain, M. I., Faruque, M. R. I., Islam, M. T. and Ullah, M. H., A new wide-band double-negative metamaterial for C- and S-B and applications. *Materials*, 2015, **8**, 57–71.
12. Sarkhel, A., Mitra, D., Paul, S. and Ranjan, S., A compact meta-atom for dual band negative permittivity metamaterial. *Microw. Opt. Technol.. Lett.*, 2015, **57**(5), 1152–1156.
13. Hasan, M. M., Faruque, M. R. I. and Islam, M. T., Inverse E-shape chiral metamaterial for long distance telecommunication. *Microw. Opt. Technol. Lett.*, 2017, **59**, 1772–1776.
14. Hasan, M. M., Faruque, M. R. I. and Islam, M. T., Compact left-handed meta-atom for S-, C- and Ku-band application. *Appl. Sci.*, 2017, **7**, 1–20.
15. Kaiser, K. L., *Electromagnetic Compatibility Handbook*, CRC Press, 2004.

Received 17 April 2017; accepted 11 April 2018

doi: 10.18520/cs/v114/i12/2518-2524